RADIOCARBON, Vol 54, Nr 2, 2012, p 165–186

THE MARINE RADIOCARBON BOMB PULSE ACROSS THE TEMPERATE NORTH ATLANTIC: A COMPILATION OF $\Delta^{14}C$ TIME HISTORIES FROM *ARCTICA ISLANDICA* GROWTH INCREMENTS

James D Scourse[1,2] • Alan D Wanamaker Jr[3] • Chris Weidman[4] • Jan Heinemeier[5] • Paula J Reimer[6] • Paul G Butler[1] • Rob Witbaard[7] • Christopher A Richardson[1]

ABSTRACT. Marine radiocarbon bomb-pulse time histories of annually resolved archives from temperate regions have been underexploited. We present here series of $\Delta^{14}C$ excess from known-age annual increments of the long-lived bivalve mollusk *Arctica islandica* from 4 sites across the coastal North Atlantic (German Bight, North Sea; Tromsø, north Norway; Siglufjordur, north Icelandic shelf; Grimsey, north Icelandic shelf) combined with published series from Georges Bank and Sable Bank (NW Atlantic) and the Oyster Ground (North Sea). The atmospheric bomb pulse is shown to be a step-function whose response in the marine environment is immediate but of smaller amplitude and which has a longer decay time as a result of the much larger marine carbon reservoir. Attenuation is determined by the regional hydrographic setting of the sites, vertical mixing, processes controlling the isotopic exchange of ^{14}C at the air-sea boundary, ^{14}C content of the freshwater flux, primary productivity, and the residence time of organic matter in the sediment mixed layer. The inventories form a sequence from high magnitude-early peak (German Bight) to low magnitude-late peak (Grimsey). All series show a rapid response to the increase in atmospheric $\Delta^{14}C$ excess but a slow response to the subsequent decline resulting from the succession of rapid isotopic air-sea exchange followed by the more gradual isotopic equilibration in the mixed layer due to the variable marine carbon reservoir and incorporation of organic carbon from the sediment mixed layer. The data constitute calibration series for the use of the bomb pulse as a high-resolution dating tool in the marine environment and as a tracer of coastal ocean water masses.

INTRODUCTION

Thermonuclear weapons testing in the 1950s and 1960s approximately doubled the amount of radiocarbon in the atmosphere compared to pre-bomb levels (Goodsite et al. 2001). This atmospheric excess ^{14}C "bomb pulse" is registered in both inorganic and organic materials as carbon is cycled through natural systems and is reported as $\Delta^{14}C$, the deviation of a sample $^{14}C/^{12}C$ ratio from its pre-industrial level expressed in per mil (‰) (Mahadevan 2001). The ^{14}C bomb pulse is therefore an exceptionally important environmental tracer and has been used in diverse applications in both terrestrial and marine settings. With an equilibration time of 7–10 yr (Mahadevan 2001), ^{14}C infuses into the ocean through air-sea gas exchange. The mixing of carbon of different ages as water masses evolve, notably linked to the depletion through radioactive decay in deep-water reservoirs isolated from the atmosphere (Broecker and Peng 1982), means that $\Delta^{14}C$ can be used as an important tracer for water mass circulation (e.g. Broecker et al. 1980; Wunsch 1984; Sikes et al. 2008; Wanamaker et al. 2012) and as a tool for assessing air-sea CO_2 exchange (Gruber 1998; Sweeney et al. 2007; Müller et al. 2008).

^{14}C measurements from known-age increments of near-surface annually banded corals covering the past 60 yr from subtropical and tropical contexts have provided valuable records of the marine expression of the bomb pulse (Druffel 1987, 1989, 1997; Toggweiler et al. 1991; Guilderson and Schrag 1998; Guilderson et al. 1998, 2000; Druffel et al. 2008; Reimer et al. 2009) with significant

[1]School of Ocean Sciences, College of Natural Sciences, Bangor University, Bangor LL59 5AB, United Kingdom.
[2]Corresponding author. Email: j.scourse@bangor.ac.uk.
[3]Department of Geological and Atmospheric Sciences, 253 Science I, Iowa State University, Ames, Iowa 50011-3212, USA.
[4]Waquoit Bay National Estuarine Research Reserve, PO Box 3092, 149 Waquoit Highway, Waquoit, Massachusetts 02536, USA.
[5]AMS ^{14}C Dating Centre, Department of Physics and Astronomy, Aarhus University, DK-8000 Aarhus C, Denmark.
[6]^{14}CHRONO Centre, Queen's University Belfast, Belfast BT7 1NN, Northern Ireland, United Kingdom.
[7]Department of Marine Ecology, Royal Netherlands Institute for Sea Research (NIOZ), PO Box 59, 1790 AB Den Burg, Texel, the Netherlands.

ocean circulation applications (e.g. Grumet et al. 2002; Hua et al. 2005; Kilbourne et al. 2007). Mahadevan (2001) compared $\Delta^{14}C$ time histories from annually banded corals with one-dimensional model simulations to discriminate between advection, air-sea flux, convection, and diffusion as controls of $\Delta^{14}C$ in surface waters across the Pacific Ocean. $\Delta^{14}C$ records can also be used as calibration series for very high-resolution dating of marine sediment sequences (e.g. Ohkouchi et al. 2003). These applications have hitherto been largely confined to the availability of suitable coral from subtropical and tropical sites, and have been restricted in temperate shelf seas because of the lack of an annually resolved archive yielding known-age increments suitable for ^{14}C analysis. Temperate or high-latitude $\Delta^{14}C$ profiles have generally been used in the inverse sense, applied to non-annually resolved archives in order to assess rate of growth, to validate organism age (e.g. Kalish et al. 2001; Ardizzone et al. 2006; Campana et al. 2008), and/or to ascertain whether increments are indeed annual in period or not (e.g. Sherwood et al. 2005; Kilada et al. 2007, 2009; Sherwood and Edinger 2009). Recently, however, $\Delta^{14}C$ time histories from cold-water corals from the temperate and northern North Atlantic have been used to reconstruct mixing and regional hydrography (e.g. Sherwood et al. 2008).

Weidman and Jones (1993) presented a time history of bomb ^{14}C on Georges Bank (NW Atlantic) using known-age increments from the annually banded long-lived marine mollusk *Arctica islandica*. Measurements from a 54-yr-old specimen live-collected in 1990 enabled a time history of $\Delta^{14}C$ from 1939 to 1990. In comparison with 2 North Atlantic coral-derived $\Delta^{14}C$ inventories (Druffel 1989), the depleted $\Delta^{14}C$ values from this site revealed "old" Labrador Sea water as a significant component of Georges Bank water and were used to constrain models suggesting a reduction in Labrador Sea (deep) Water formation during the late 1960s and 1970s. Witbaard et al. (1994) used $\Delta^{14}C$ profiles from *A. islandica* from the Oyster Ground, southern North Sea, along the seasonal $\delta^{18}O$ profiles, to verify that the increments in this species are annual in period. Given that the annual period for the major increment formation in *A. islandica* is now well established (Murawski et al. 1982; Weidman et al. 1994; Schöne et al. 2005), the $\Delta^{14}C$ record from the Oyster Ground series can also be interpreted as an indicator of hydrographic variability.

These studies demonstrated the potential for $\Delta^{14}C$ time histories from *A. islandica* to identify spatial gradients in temperate to subpolar hydrographic variability and air-sea gas exchange, but they have not been followed by similar studies from other regions of the North Atlantic. This is surprising given the significance of the subpolar North Atlantic as a primary source of deep water contributing to the global thermohaline circulation, and the existence of abundant populations of *A. islandica* across the temperate and boreal North Atlantic (Dahlgren et al. 2000) adjacent to sites of North Atlantic Deep Water convection.

We present here $\Delta^{14}C$ series measured on known-age annual increments of *A. islandica* from across the temperate North Atlantic, from sites on the north Icelandic shelf (2 series; Grimsey and Siglufjordur), the southern North Sea (German Bight), and northern Norway (Tromsø). These are combined with published *A. islandica* $\Delta^{14}C$ series from Georges Bank, NW Atlantic (Weidman and Jones 1993); Sable Bank, NW Atlantic (Kilada et al. 2007); and from the Oyster Ground, southern North Sea (Witbaard et al. 1994) (Figure 1).

The north Icelandic shelf is dominated by oceanic water masses. At present, the North Atlantic Polar Front (NAPF) extends across the north Icelandic shelf (e.g. Ólafsson 1999; Rytter et al. 2002), separating easterly flowing warm and high-salinity Atlantic Water (Irminger Current) from Arctic Surface Water (Johannessen 1986), a cold low-salinity water mass derived from modified Polar Water of the East Icelandic and East Greenland currents (Figure 1). At shallow depths down to 300–400 m, including the *A. islandica* sampling stations reported here, the Atlantic water extends to the

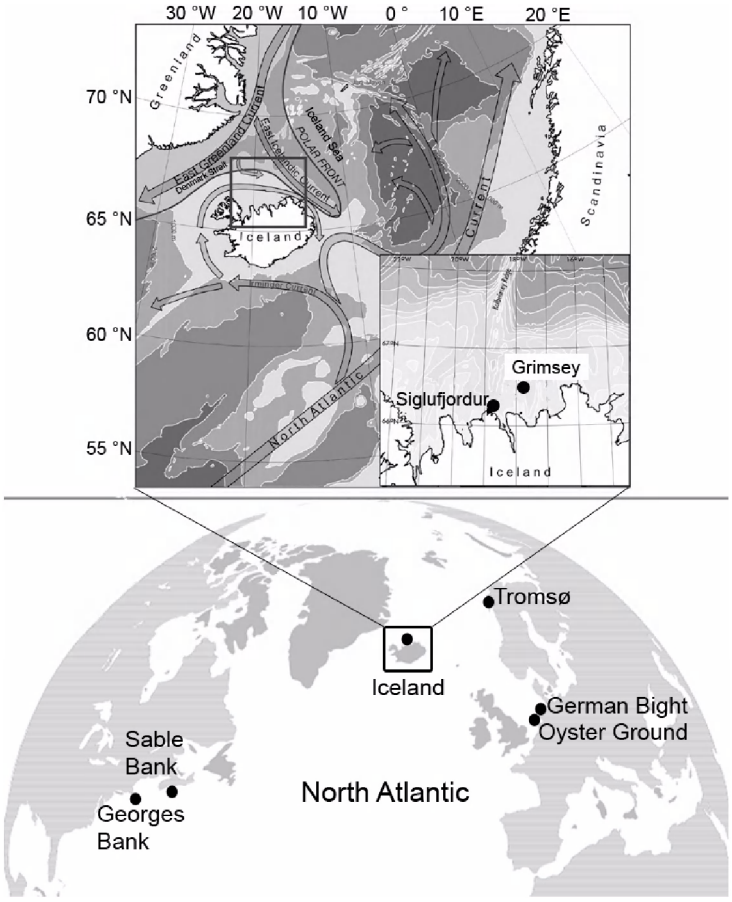

Figure 1 Location map of the North Atlantic showing all sites referred to in the text and detail of the north Icelandic shelf.

seabed (cf. Stefánsson 1962; Knudsen and Eiríksson 2002; Knudsen et al. 2004; Eiríksson et al. 2011) and stratifies during the summer months (Eiríksson et al. 2011). Over recent decades, however, well-instrumented temperature-salinity anomalies, in particular the Great Salinity Anomaly (GSA) during the 1960s (Dickson et al. 1988; Sundby and Drinkwater 2007), have resulted in cold low-salinity Arctic waters reaching the north Icelandic coast, displacing the NAPF south of the entire northern shelf and generating winter sea ice cover between Iceland and Greenland. Hydrographic data indicate that during the GSA, Arctic Water extended to the seabed, displacing Atlantic Water across the north Icelandic shelf. The East Icelandic Current is characterized by depleted ^{14}C values (Tauber and Funder 1975; Eiríksson et al. 2011) with $\Delta R \approx +200$ yr (ΔR is defined as the regional offset from the global marine model age at any given point in time, i.e. the measured ^{14}C age of a sample of known age minus the marine calibration curve age at that [calendar] time; Stuiver and Brazunias 1993); hence, a decrease in $\Delta^{14}C$ might be expected in this region during the GSA. Both north Icelandic shelf sites are close to normal fully marine salinities; Siglufjordur has a smaller drainage basin than most fjords in north Iceland, receiving little water from central Iceland or glacial meltwater. The Tromsø sample was collected from very shallow depths (3 m, surface mixed layer) in a fjordic setting strongly influenced by the inflow of North Atlantic surface water via the North Atlantic Current and the Norwegian Coastal Current. The shelf

waters on the southern flank of Georges Bank from where the analyzed specimen was recovered consist of 75% Scotian Shelf Water and 25% Slope Water, both of which are southerly flowing cold water masses that originate in the Labrador Sea (Chapman and Beardsley 1989; Weidman and Jones 1993); water masses of similar origin dominate Sable Bank to the north (Hannah et al. 2001).

The shallow North Sea (<200 m) is preconditioned by warm saline Atlantic Water (90%) flowing via the Shetland Current and through the Strait of Dover with the remainder consisting of freshwater inputs from riverine sources (e.g. Rhine, Thames), brackish inputs from the Baltic Sea outflow, and precipitation (Hardisty 1990). The dominant outflow from the North Sea is via the Norwegian Coastal Current. The hydrography in the North Sea is dominated by high tidal and wave energy levels; the shallower sites, such as the German Bight, are therefore very well mixed, but in the summer deeper northern areas such as the Oyster Ground become stratified (Weston et al. 2008), separated from the mixed sector by the development of the seasonal southern North Sea tidal mixing front (Hill et al. 1993). The German Bight is also strongly influenced by riverine inputs, notably from the Elbe, which significantly reduces the salinity in the German Bight (29–31) compared with the Oyster Ground (33–35; Witbaard et al. 1994). The southern North Sea sites therefore range from fully mixed and strongly coastal (German Bight) to seasonally stratified open shelf (Oyster Ground).

The aims of this paper are 1) to present this compilation of % modern carbon (pMC) time histories as a basis for identifying the regional variability in $\Delta^{14}C$, and therefore age and mixing histories, of coastal waters across the North Atlantic; 2) to test the hypothesis that the Great Salinity Anomaly (GSA) of the north Icelandic shelf during the 1960s is detectable as a plateau or reduction in ^{14}C excess; and 3) to assess these data as calibration series for ultra high-resolution ^{14}C dating of shallow marine sediment records.

MATERIALS AND METHODS

The *A. islandica* shell is deposited as a series of annual growth increments (fast growth) separated by narrow growth checks (slow growth or cessation of growth) (Figure 2; Jones 1983). The longevity of the species is well in excess of the ~60 yr required to provide increments covering the atmospheric bomb pulse from single live-collected specimens; an exceptional live-collected specimen from the north Icelandic shelf has been determined to be 507 yr old, making it likely the longest-lived non-colonial animal known to science (Butler et al. 2012). The Georges Bank series is based on the analysis of a single live-collected individual (Weidman and Jones 1993). However, annual growth increment width declines with age, forming a clear ontogenetic growth trend (Figure 2). Often, the individual senescent annual growth increments are too small for ^{14}C subsampling, given the minimum weight of aragonite required for high-precision accelerator mass spectrometry (AMS) ^{14}C analysis (~10 mg), and subsampling of the early, wide, juvenile increments is preferred. This can be achieved by analysis of a number of live-collected individuals of different age that settled sequentially during the course of the bomb-pulse period. The series reported here are based on analyses of single live-collected specimens, apart from the Grimsey (collected 2006, north Icelandic shelf) and published Oyster Ground (collected 1988; Witbaard et al. 1994) series, which are based on analyses of a number of live-collected specimens of similar collection dates but differing longevities.

The live-collected *A. islandica* specimens used in this analysis were collected from shallow marine settings (3–80 m water depths) from sites in north Norway (Tromsø), the German Bight of the southern North Sea, and the north Icelandic shelf (Grimsey and Siglufjordur; Figure 1; Table 1). For the Tromsø, German Bight, and Siglufjordur samples, specimen ages were determined by increment counting as described by Ropes (1984). Specimens of suitable longevity were selected and prepared by radially sectioning a 2-mm-thick slice from 1 valve (Weidman and Jones 1993). The perio-

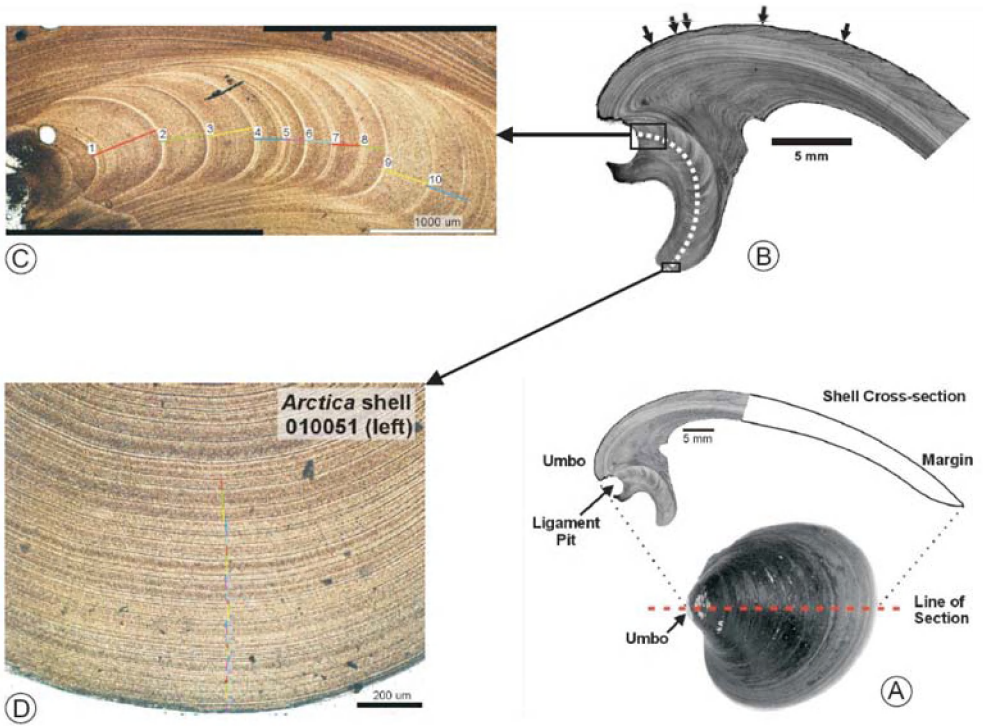

Figure 2 (adapted from Scourse et al. 2006). (A) *Arctica islandica* external valve face, showing line of section through valve. (B) Acetate peel replica cross-section of valve showing annual growth band increments along shell margin (arrows) and within hinge-plate. The axis of growth through the hinge plate used to generate increment data is indicated by the dashed white line. (C) Numbered annual growth bands are measured from the earliest growth bands to the most recent along the axis of growth. Juvenile early bands are wide and reflect the ontogenetic growth curve of the individual. (D) Narrow senescent late bands from the outer part of the hinge plate axis with youngest increment at base.

stracum (outer organic layer) and the nacre (inner laminated aragonite layer) were ground away to reveal the central prismatic layer (growth banded aragonite), which was then subsectioned into samples containing 1 to 3 annual increments. The number of annual bands integrated into individual samples was determined by the minimum amount of aragonite required for AMS ^{14}C analysis. Temporal resolution was reduced in the more recently deposited increments because of the ontogenetic growth trend. For the Grimsey (north Icelandic shelf) shells (Figure 1), live-caught animals were harvested, sectioned, and prepared for image analysis (increment counting) following methods outlined by Scourse et al. (2006). Approximately a 30-mg solid sample of shell aragonite was removed from the desired increment (calendar year) from the outer shell surface (Figure 2) using a razor blade. Prior to ^{14}C sampling, the periostracum was physically removed with a razor blade. Each sample taken for ^{14}C analysis represented 1 year's growth. The age assignment of each ^{14}C sample was determined by counting the last complete annual increment (representing 2005) on each shell, back to the targeted increment. The individuals used from Grimsey have been absolutely dated by cross-dating techniques (Butler et al. 2012).

The Tromsø, German Bight, and Siglufjordur samples were prepared for AMS ^{14}C analysis by first etching in 10% HCl for 30 seconds to remove surface contaminants, followed by conversion to CO_2 in anhydrous phosphoric acid at 60 °C (overnight), and finally conversion to graphite using a hydrogen reduction and iron catalytic process (Gagnon and Jones 1993). Graphite targets were analyzed

Table 1 Details of *Arctica islandica* sample collection sites.

Site	Location	Water depth (m)	Year of collection	Nr of specimens	Measurements per specimen
North Norway, Tromsø	70°N, 19°E	3	1993	1	14
German Bight, southern North Sea	54°N, 7°E	37	1990	2	7–13
Oyster Ground, southern North Sea (Witbaard et al. 1994)	54°N, 4°E	30–50	1988	2	5–13
North Icelandic shelf, Siglufjordur	66°N, 19°W	22	1991	3	4–7
North Icelandic shelf, Grimsey	66°N, 18°W	80	2006	6	1–6
Georges Bank, NW Atlantic (Weidman and Jones 1993)	41°N, 67°W	76	1990	1	13
Sable Bank (Kilada et al. 2007)	44°N, 61°W	33–70	2003	6	2–3

at the National Ocean Sciences AMS Facility at Woods Hole Oceanographic Institution, Woods Hole, Massachusetts, USA. Analytical $\Delta^{14}C$ error for these samples ranged from ±3.0‰ to ±13.5‰ with a mean of ±5.7‰. The Grimsey samples were treated following a standard mollusk pretreatment procedure and measured using the EN tandem accelerator at the University of Aarhus (Denmark). To eliminate any possible surface contamination, the outer 10–25% of the shell was removed by etching in weak HCl (for sample size >8 mg carbonate) after ultrasonic rinsing. Any organic carbon incorporated in the shell carbonate was removed by treatment with a $KMnO_4$ solution for 16–20 hr at 80 °C. The CO_2 was liberated with ~100% phosphoric acid in an evacuated vial at 25 °C. Part of the CO_2 was used for $\delta^{13}C$ measurements; the rest was converted to graphite for AMS ^{14}C measurements by reduction with H_2, with cobalt as a catalyst (Vogel et al. 1984). $\Delta^{14}C$ data are age-corrected to AD 1950 and normalized to a $\delta^{13}C$ (VPDB) value of –25‰ (Andersen et al. 1989), according to the methods outlined by Stuiver and Polach (1977). To correct for natural isotopic fractionation, $\delta^{13}C$ values were obtained either from subsamples of the same material analyzed for $\Delta^{14}C$, interpolation with adjacent samples from within the same shell, or the mean $\delta^{13}C$ of other *A. islandica* shells in the region. *A. islandica* shell $\delta^{13}C$ values averaged about +2‰. Data are given in Table 2 in pMC, which is corrected for natural isotopic fractionation and is equivalent to $F^{14}C \times 100\%$ (Reimer et al. 2004).

In order to compare our recent AMS ^{14}C results with previous studies (e.g. Weidman and Jones 1993), we converted age-corrected $\Delta^{14}C$ (Δ in conventional notation) into pMC values using the following equation, which can be derived from the equations of Stuiver and Polach (1977), where x is the growth increment sample calendar year AD:

$$pMC = (1 + \Delta^{14}C/1000)\, e^{-(1950-x)/8267} \times 100\% \quad (1)$$

Note that $\Delta^{14}C$ is age-corrected in this equation. ΔR was determined by comparing the measured ^{14}C age with the ^{14}C value of the Marine09 calibration curve or modeled marine bomb pulse (Reimer et al. 2009) for the increment year concerned (cf. Wanamaker et al. 2008, 2012; Butler et al. 2012).

RESULTS

The data generate $\Delta^{14}C$ time histories for the marine bomb pulse for the regions investigated (Figure 3; Table 2), which can be compared with the modeled global marine surface mixed-layer bomb pulse (Reimer et al. 2009). The marine curve is highly correlated at all sites but damped with respect to the atmospheric signal, and the amplitude of the marine peak differs in a number of key respects between regions. As noted by Weidman and Jones (1993), the Georges Bank signal contains reduced

$\Delta^{14}C$ excess, reaching a 1974 peak of 108 pMC, in comparison with the Bermuda and Florida coral records (Druffel 1989), both of which reach ~115 pMC. The Sable Bank data (Kilada et al. 2007) are quite noisy, probably a reflection that a number of different individuals from a range of depths have been sampled, but in general this data set plots very close to the Georges Bank data with a peak of 109 pMC in 1968. However, the north Icelandic shelf series are characterized by an even more attenuated $\Delta^{14}C$ excess signal than at Georges and Sable banks, with peaks of 106 pMC (Siglufjordur) at 1971 and 104 pMC (Grimsey) in 1980. The Grimsey data show the lowest $\Delta^{14}C$ excess of all series analyzed from across the temperate North Atlantic. The Tromsø data show a larger excess, with a double peak at 1970 (~113 pMC) and 1977 (~112 pMC). The largest excess recorded is from the North Sea, the German Bight series reaching an initial peak of ~124 pMC in 1968. The Oyster Ground (southern North Sea) series is slightly attenuated compared with the German Bight, but has a double peak with maxima of ~121 pMC in 1966 and 1974 (Witbaard et al. 1994); the differences in the timing of the peaks in the Oyster Ground and German Bight series are within the sampling error. The Tromsø series is very close to the modeled surface ocean bomb pulse (Reimer et al. 2009); the large excess of the 2 North Sea series lie between the modeled surface ocean values and the atmospheric signal, while those from the more oceanic Georges and Sable banks and the north Icelandic shelf sites lie well below the surface ocean model values.

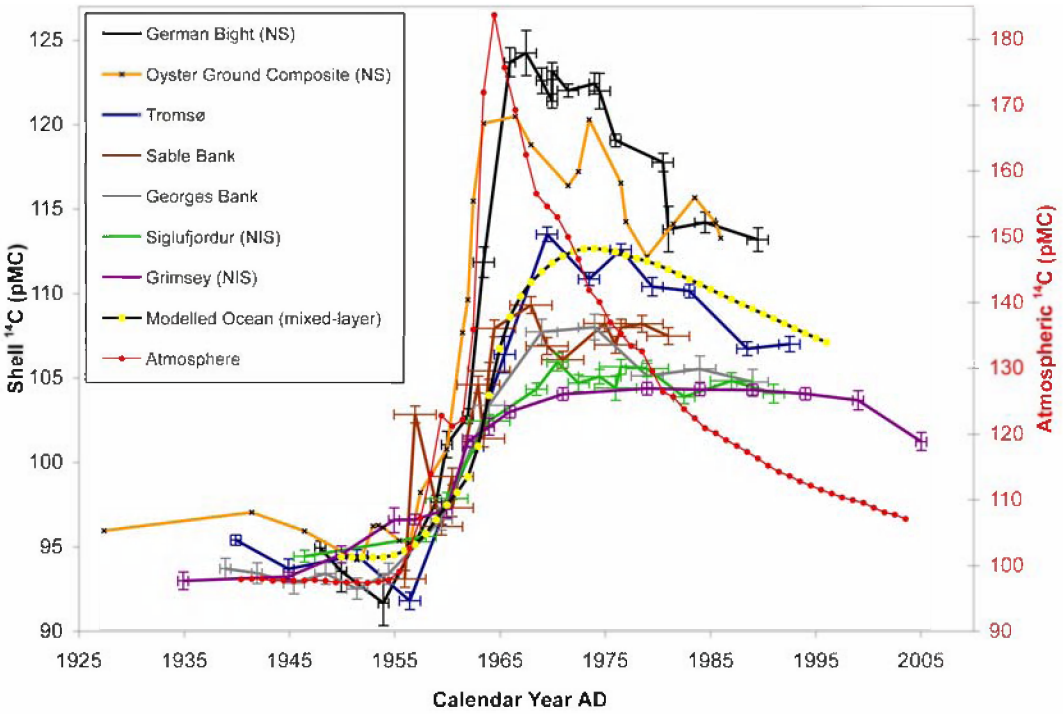

Figure 3 Radiocarbon data from all sites expressed as pMC plotted against the absolute date AD. The Grimsey, Siglufjordur, German Bight, and Tromsø data are published for the first time here, though the Siglufjordur, German Bight, and Tromsø data are presented in Weidman (1995); the series from Georges Bank (Weidman and Jones 1993), Oyster Ground (Witbaard et al. 1994), and Sable Bank (Kilada et al. 2007) have been published previously. The Northern Hemisphere atmospheric bomb pulse (Levin and Kromer 2004; Levin et al. 2008) and the modeled surface ocean mixed-layer bomb pulse (Reimer et al. 2009) are shown for comparison. Analytical and dating uncertainty are shown for all data points except the Oyster Ground; for this site the data from the 3 shells analyzed have been processed using a low pass filter (Savitzky-Golay; span = 5; degree = 2) to show the "mean" response (see Table 2 for analytical and dating uncertainty based on sample resolution).

Table 2 ^{14}C data, laboratory codes, sample identification codes, and references. The ΔR values before and during the bomb pulse are calculated as the difference between the measured ^{14}C age (= 8033 ln(pMC/100)) and the age expected from the Marine09 calibration curve or the post-bomb modeled marine response (given at the end of the table (Reimer et al. 2009), respectively. The ΔR calculations are based on a moving average of the marine model data corresponding to the number of years integrated in each sample. The 1950 reference value is taken as the average of the 2 curves (* = estimated value; ΔR = ^{14}C age–Marine09).

Lab code	Sample ID	Site	Depth (m)	Year (AD)	$\Delta^{14}C$	Error (±1σ)	pMC	Error (±1σ)	$\delta^{13}C$	Error (±1σ)	SI yr[a]	ΔR	Reference
AAR-12282	273-1	Grimsey, NIS	81–83	1935	–68.6	5.2	93.03	0.52	1.39	0.05	1	120	This study
AAR-12283	273-2	Grimsey, NIS	81–83	1945	–67.2	2.7	93.28	0.27	2.18	0.05	1	95	This study
AAR-12284	280-1	Grimsey, NIS	81–83	1950	–54.8	5.0	94.58	0.5	2.05	0.05	1	–3	This study
AAR-12285	279-1	Grimsey, NIS	81–83	1955	–35.1	7.3	96.61	0.73	2.02	0.05	1	74	This study
AAR-12286	279-2	Grimsey, NIS	81–83	1957	–34.9	3.1	96.65	0.31	2.09	0.05	1	207	This study
AAR-12287	279-3	Grimsey, NIS	81–83	1960	–29.1	4.7	97.25	0.47	2.01	0.05	1	538	This study
AAR-12288	279-4	Grimsey, NIS	81–83	1962	10.4	3.4	101.24	0.34	1.88	0.05	1	565	This study
AAR-12289	279-5	Grimsey, NIS	81–83	1964	19.1	5.0	102.13	0.5	1.66	0.05	1	646	This study
AAR-12290	279-6	Grimsey, NIS	81–83	1966	27.6	3.6	103.01	0.36	1.53	0.05	1	657	This study
AAR-12291	290-1	Grimsey, NIS	81–83	1971	37.5	3.7	104.06	0.37	0.68	0.05	1	633	This study
AAR-12292	278-1	Grimsey, NIS	81–83	1979	40.0	3.8	104.38	0.38	1.60	0.05	1	544	This study
AAR-12293	278-2	Grimsey, NIS	81–83	1984	38.9	3.8	104.33	0.38	1.97	0.05	1	443	This study
AAR-12294	299-1	Grimsey, NIS	81–83	1989	37.9	3.5	104.29	0.35	1.43	0.05	1	340	This study
AAR-12295	299-2	Grimsey, NIS	81–83	1994	35.1	3.6	104.07	0.36	0.79	0.05	1	252	This study
AAR-12296	299-3	Grimsey, NIS	81–83	1999	30.6	5.6	103.69	0.56	1.64	0.05	1	NA	This study
AAR-12297	299-4	Grimsey, NIS	81–83	2005	5.9	5.4	101.26	0.54	0.68	0.05	1	NA	This study
WHG-954	GB61-7-1B	Georges Bank	76	1939	–61.3	6.2	93.75	0.62	2.30	NA	1	60	Weidman & Jones 1993
WHG-955	GB61-7-1B	Georges Bank	76	1942	–64.4	6.1	93.47	0.61	2.30	NA	1	81	Weidman & Jones 1993
WHG-959	GB61-7-1B	Georges Bank	76	1945.5	–70.6	6.2	92.89	0.62	2.30	NA	2	129	Weidman & Jones 1993
WHG-951	GB61-7-1B	Georges Bank	76	1948.5	–65.3	6.3	93.45	0.63	2.30	NA	2	77	Weidman & Jones 1993
WHG-952	GB61-7-1B	Georges Bank	76	1951.5	–74.6	6.2	92.56	0.62	2.30	NA	2	161	Weidman & Jones 1993
WHG-947	GB61-7-1B	Georges Bank	76	1954.5	–66.0	6.2	93.45	0.62	2.30	NA	2	88	Weidman & Jones 1993
WHG-949	GB61-7-1B	Georges Bank	76	1959.5	–34.4	6.4	96.67	0.64	2.30	NA	2	32	Weidman & Jones 1993
WHG-956	GB61-7-1B	Georges Bank	76	1964	32.3	6.7	103.40	0.67	2.30	NA	3	38	Weidman & Jones 1993
WHG-957	GB61-7-1B	Georges Bank	76	1969	74.8	7.4	107.73	0.74	2.30	NA	3	259	Weidman & Jones 1993
WHG-958	GB61-7-1B	Georges Bank	76	1974	77.0	7.6	108.01	0.76	2.30	NA	3	336	Weidman & Jones 1993
WHG-960	GB61-7-1B	Georges Bank	76	1979	47.7	7.5	105.14	0.75	2.30	NA	3	500	Weidman & Jones 1993
WHG-962	GB61-7-1B	Georges Bank	76	1984	51.1	7.7	105.54	0.77	2.30	NA	3	372	Weidman & Jones 1993
WHG-961	GB61-7-1B	Georges Bank	76	1989	42.8	7.4	104.77	0.74	2.30	NA	3	323	Weidman & Jones 1993
OS-2667	2667	Siglufjordur, NIS	22	1874	–55.0	3.5	93.64	0.35	2.60	NA	1	53	Weidman 1995
OS-2666	2666	Siglufjordur, NIS	22	1894	–53.8	3.3	93.98	0.33	2.50	NA	1	39	Weidman 1995
OS-2665	2665	Siglufjordur, NIS	22	1916.5	–59.5	3.5	93.67	0.35	1.90	NA	2	77	Weidman 1995

Table 2 ^{14}C data, laboratory codes, sample identification codes, and references. The ΔR values before and during the bomb pulse are calculated as the difference between the measured ^{14}C age (= 8033 ln(pMC/100)) and the age expected from the Marine09 calibration curve or the post-bomb modeled marine response (given at the end of the table (Reimer et al. 2009), respectively. The ΔR calculations are based on a moving average of the marine model data corresponding to the number of years integrated in each sample. The 1950 reference value is taken as the average of the 2 curves (* = estimated value; ΔR = ^{14}C age–Marine09). *(Continued)*

Lab code	Sample ID	Site	Depth (m)	Year (AD)	$\Delta^{14}C$	Error (±1σ)	pMC	Error (±1σ)	$\delta^{13}C$	Error (±1σ)	SI yr[a]	ΔR	Reference
OS-2664	2664	Siglufjordur, NIS	22	1946.5	–54.8	3.8	94.48	0.38	1.80	NA	2	–9	Weidman 1995
OS-2736	2736	Siglufjordur, NIS	22	1958	–44.4	3.6	95.65	0.36	1.90	NA	1	13	Weidman 1995
OS-2733	2733	Siglufjordur, NIS	22	1960	–22.3	5.3	97.89	0.53	1.80	NA	1	–32	Weidman 1995
OS-2731	2731	Siglufjordur, NIS	22	1964	22.9	4.9	102.46	0.49	2.60	NA	1	119	Weidman 1995
OS-2734	2734	Siglufjordur, NIS	22	1968.5	41.1	4.3	104.34	0.43	2.30	NA	2	493	Weidman 1995
OS-2730	2730	Siglufjordur, NIS	22	1970.5	56.9	7.3	105.95	0.73	2.00	NA	2	446	Weidman 1995
OS-2735	2735	Siglufjordur, NIS	22	1972.5	44.2	4.4	104.70	0.44	1.80	NA	2	581	Weidman 1995
OS-2672	2672	Siglufjordur, NIS	22	1974.5	47.8	4.8	105.09	0.48	1.30	NA	2	556	Weidman 1995
OS-2671	2671	Siglufjordur, NIS	22	1976	40.8	4.1	104.41	0.41	1.70	NA	1	596	Weidman 1995
OS-2732	2732	Siglufjordur, NIS	22	1976.5	53.3	4.8	105.67	0.48	1.70	NA	2	493	Weidman 1995
OS-2669	2669	Siglufjordur, NIS	22	1979	51.9	5.5	105.56	0.55	1.90	NA	1	469	Weidman 1995
OS-2673	2673	Siglufjordur, NIS	22	1982.5	34.9	6.1	103.90	0.61	1.90	NA	2	530	Weidman 1995
OS-2670	2670	Siglufjordur, NIS	22	1987	43.7	4.4	104.84	0.44	1.80	NA	1	361	Weidman 1995
OS-2668	2668	Siglufjordur, NIS	22	1991	35.7	4.2	104.08	0.42	1.60	NA	1	334	Weidman 1995
OS-0093	N-8A	German Bight	37	1948	–50.0	3.9	94.98	0.39	2.00	NA	1	–53	Weidman 1995
OS-0094	N-8A	German Bight	37	1950	–64.1	12.2	93.59	1.22	2.00	NA	1	68	Weidman 1995
rec#1018	N-8A	German Bight	37	1954	–83.3	13.2	91.71	1.32	2.00	NA	1	234	Weidman 1995
OS-0090	N-8A	German Bight	37	1959	–24.2	3.9	97.69	0.39	2.00	NA	1	–86	Weidman 1995
OS-1351	N-8A II	German Bight	37	1960	9.5	7.8	101.07	0.78	2.00	NA	1	–289	Weidman 1995
OS-0089	N-8A	German Bight	37	1962	26.2	4.3	102.77	0.43	2.00	NA	1	–286	Weidman 1995
OS-1349	N-8A II	German Bight	37	1963.5	116.6	9.1	111.84	0.91	2.00	NA	2	–703	Weidman 1995
OS-0130	N1-B	German Bight	37	1966	234.2	8.5	123.66	0.85	2.00	NA	1	–1042	Weidman 1995
OS-1350	N-8A II	German Bight	37	1967.5	239.3	13.3	124.19	1.33	2.00	NA	2	–956	Weidman 1995
OS-0128	N1-B	German Bight	37	1969	222.8	7.6	122.56	0.76	2.00	NA	1	–775	Weidman 1995
OS-0091	N-8A	German Bight	37	1970	210.7	4.1	121.36	0.41	2.00	NA	1	–660	Weidman 1995
OS-0642	N1-B	German Bight	37	1970	228.4	5.0	123.14	0.5	2.00	NA	1	–777	Weidman 1995
OS-1424	N-8A II	German Bight	37	1971.5	216.7	3.8	121.99	0.38	2.00	NA	2	–662	Weidman 1995
OS-0099	N1-B	German Bight	37	1974	220.4	6.2	122.39	0.62	2.00	NA	1	–666	Weidman 1995
OS-0088	N-8A	German Bight	37	1974.5	216.0	10.5	121.96	1.05	2.00	NA	2	–640	Weidman 1995
OS-1400	N-8A II	German Bight	37	1976	186.7	3.7	119.04	0.37	2.00	NA	1	–457	Weidman 1995
OS-0097	N1-B	German Bight	37	1980.5	173.0	5.4	117.73	0.54	2.00	NA	2	–433	Weidman 1995
OS-0087	N-8A	German Bight	37	1981	133.7	13.5	113.80	1.35	2.00	NA	1	–169	Weidman 1995

Table 2 ^{14}C data, laboratory codes, sample identification codes, and references. The ΔR values before and during the bomb pulse are calculated as the difference between the measured ^{14}C age (= 8033 ln(pMC/100)) and the age expected from the Marine09 calibration curve or the post-bomb modeled marine response (given at the end of the table (Reimer et al. 2009), respectively. The ΔR calculations are based on a moving average of the marine model data corresponding to the number of years integrated in each sample. The 1950 reference value is taken as the average of the 2 curves (* = estimated value; ΔR = ^{14}C age–Marine09). *(Continued)*

Lab code	Sample ID	Site	Depth (m)	Year (AD)	$\Delta^{14}C$	Error (±1σ)	pMC	Error (±1σ)	$\delta^{13}C$	Error (±1σ)	SI yr[a]	ΔR	Reference
OS-0096	N1-B	German Bight	37	1984.5	137.2	6.1	114.20	0.61	2.00	NA	2	–272	Weidman 1995
OS-0131	N1-B	German Bight	37	1989.5	126.4	7.0	113.18	0.7	2.00	NA	2	–308	Weidman 1995
OS-3019	T-2A	Tromsø	3	1940	–44.5	3.0	95.43	0.3	2.50	NA	1	–85	Weidman 1995
OS-3018	T-2A	Tromsø	3	1945	–62.2	5.8	93.72	0.58	2.40	NA	1	57	Weidman 1995
OS-3017	T-2A	Tromsø	3	1951.5	–54.7	3.1	94.55	0.31	2.50	NA	2	–11	Weidman 1995
OS-3016	T-2A	Tromsø	3	1956.5	–82.3	5.0	91.84	0.5	2.50	NA	2	271	Weidman 1995
OS-3015	T-2A	Tromsø	3	1959.5	–34.2	3.5	96.69	0.35	1.80	NA	2	32	Weidman 1995
OS-2865	T-2A	Tromsø	3	1962.5	8.0	3.2	100.95	0.32	1.90	NA	2	–70	Weidman 1995
rec #-6163	T-2A	Tromsø	3	1965.5	61.9	10.7	106.39	1.07	2.10	NA	2	96	Weidman 1995
OS-2864	T-2A	Tromsø	3	1969.5	132.2	4.3	113.49	0.43	1.80	NA	2	–139	Weidman 1995
OS-2863	T-2A	Tromsø	3	1973.5	105.3	3.8	110.84	0.38	2.10	NA	2	129	Weidman 1995
OS-2852	T-2A	Tromsø	3	1976.5	122.3	3.3	112.59	0.33	1.80	NA	2	–17	Weidman 1995
OS-2851	T-2A	Tromsø	3	1979.5	100.0	5.4	110.39	0.54	1.70	NA	2	102	Weidman 1995
OS-3527	T-2A	Tromsø	3	1983	97.0	4.0	110.14	0.4	1.70	NA	1	50	Weidman 1995
OS-2738	T-2A	Tromsø	3	1988.5	62.4	4.0	106.74	0.4	1.50	NA	2	184	Weidman 1995
OS2737	T-2A	Tromsø	3	1992.5	64.6	4.5	107.01	0.45	1.30	NA	2	80	Weidman 1995
UTC-1070	RWL-7	Oyster Ground	30–50	1986	147	8	115.20	0.8	1.50	NA	5	–375	Witbaard et al. 1994
UTC-1013	RWL-7	Oyster Ground	30–50	1983.5	157	7	116.17	0.7	1.46	NA	10	–390	Witbaard et al. 1994
UTC-1071	RWL-7	Oyster Ground	30–50	1977	136	10	113.97	1	1.50	NA	6	–354	Witbaard et al. 1994
UTC-1072	RWL-7	Oyster Ground	30–50	1972.5	168	14	117.12	1.4	1.07	NA	6	–331	Witbaard et al. 1994
UTC-1073	RWL-7	Oyster Ground	30–50	1966.5	180	13	118.24	1.3	1.67	NA	6	–691	Witbaard et al. 1994
UTC-1074	RWL-7	Oyster Ground	30–50	1961.5	–16	7	98.54	0.7	1.85	NA	6	69	Witbaard et al. 1994
UTC-1075	RWL-7	Oyster Ground	30–50	1956.5	–45	8	95.58	0.8	1.80	NA	6	–29	Witbaard et al. 1994
UTC-1014	RWL-7	Oyster Ground	30–50	1953.5	–25	8	97.54	0.8	1.29	NA	6	–254	Witbaard et al. 1994
UTC-1076	RWL-7	Oyster Ground	30–50	1951.5	–64	8	93.62	0.8	1.30	NA	6	69	Witbaard et al. 1994
UTC-1077	RWL-7	Oyster Ground	30–50	1946.5	–58	7	94.16	0.7	1.77	NA	6	19	Witbaard et al. 1994
UTC-1015	RWL-7	Oyster Ground	30–50	1941.5	–15	9	98.40	0.9	2.55	NA	6	–330	Witbaard et al. 1994
UTC-1016	RWL-7	Oyster Ground	30–50	1927.5	–39	6	95.84	0.6	2.03	NA	4	–113	Witbaard et al. 1994
UTC-2712	Shell 140	Oyster Ground	30–50	1985.5	129	7	113.39	0.7	2*	NA	6	–237	Witbaard et al. 1994
UTC-2711	Shell 140	Oyster Ground	30–50	1979	105	10	110.89	1	2*	NA	7	–157	Witbaard et al. 1994
UTC-2710	Shell 140	Oyster Ground	30–50	1973.5	203	7	120.64	0.7	2*	NA	4	–555	Witbaard et al. 1994
UTC-2709	Shell 140	Oyster Ground	30–50	1968	201	7	120.36	0.7	2*	NA	7	–922	Witbaard et al. 1994

Table 2 ^{14}C data, laboratory codes, sample identification codes, and references. The ΔR values before and during the bomb pulse are calculated as the difference between the measured ^{14}C age (= 8033 ln(pMC/100)) and the age expected from the Marine09 calibration curve or the post-bomb modeled marine response (given at the end of the table (Reimer et al. 2009), respectively. The ΔR calculations are based on a moving average of the marine model data corresponding to the number of years integrated in each sample. The 1950 reference value is taken as the average of the 2 curves (* = estimated value; ΔR = ^{14}C age–Marine09). *(Continued)*

Lab code	Sample ID	Site	Depth (m)	Year (AD)	$\Delta^{14}C$	Error (±1σ)	pMC	Error (±1σ)	$\delta^{13}C$	Error (±1σ)	SI yr[a]	ΔR	Reference
UTC-2708	Shell 140	Oyster Ground	30–50	1963.5	213	7	121.50	0.7	2*	NA	2	–1368	Witbaard et al. 1994
UTC-2707	Shell 140	Oyster Ground	30–50	1962.5	138	9	113.97	0.9	2*	NA	2	–1045	Witbaard et al. 1994
UTC-2706	Shell 140	Oyster Ground	30–50	1962	171	12	117.27	1.2	2*	NA	1	–1346	Witbaard et al. 1994
UTC-2705	Shell 140	Oyster Ground	30–50	1960	40	10	104.13	1	2*	NA	3	–531	Witbaard et al. 1994
UTC-2704	Shell 140	Oyster Ground	30–50	1957.5	–44	14	95.69	1.4	2*	NA	2	–17	Witbaard et al. 1994
UTC-2703	Shell 140	Oyster Ground	30–50	1955.5	–45	8	95.56	0.8	2*	NA	2	–75	Witbaard et al. 1994
UTC-2702	Shell 140	Oyster Ground	30–50	1954	–44	7	95.65	0.7	2*	NA	1	–104	Witbaard et al. 1994
UTC-2701	Shell 140	Oyster Ground	30–50	1953	–46	12	95.43	1.2	2*	NA	1	–86	Witbaard et al. 1994
UTC-2700	Shell 140	Oyster Ground	30–50	1952	–51	15	94.92	1.5	2*	NA	1	–42	Witbaard et al. 1994
UTC-1078	Shell RW4C	Oyster Ground	30–50	1986	114	22	111.89	2.2	0.18	NA	6	–140	Witbaard et al. 1994
UTC-1079	Shell RW4C	Oyster Ground	30–50	1981.5	142	13	114.64	1.3	1.50	NA	6	–241	Witbaard et al. 1994
UTC-1080	Shell RW4C	Oyster Ground	30–50	1976.5	166	17	116.97	1.7	1.50	NA	6	–326	Witbaard et al. 1994
UTC-1081	Shell RW4C	Oyster Ground	30–50	1971.5	139	20	114.20	2	2.81	NA	6	–144	Witbaard et al. 1994
UTC-1082	Shell RW4C	Oyster Ground	30–50	1966.5	206	6	120.84	0.6	1.83	NA	6	–866	Witbaard et al. 1994
	22A	Sable Bank	70	1963	44.6		104.62		2.27		3–4	–254	Kilada et al. 2007
	22B	Sable Bank	70	1971	58.2		106.09		1.93		3–4	447	Kilada et al. 2007
	17A	Sable Bank	33	1960.5	–9.3		99.20		3.12		3–4	–107	Kilada et al. 2007
	17B	Sable Bank	33	1964.5	77.5		107.94		3.13		3–4	–219	Kilada et al. 2007
	17C	Sable Bank	33	1976	66.3		106.97		1.72		3–4	400	Kilada et al. 2007
	19A	Sable Bank	33	1960.5	–27.9		97.33		2.75		3–4	46	Kilada et al. 2007
	19B	Sable Bank	33	1963.5	12.7		101.44		3.00		3–4	98	Kilada et al. 2007
	19C	Sable Bank	33	1975	79		108.23		2.15		3–4	316	Kilada et al. 2007
	21A	Sable Bank	33	1959.5	–38.7		96.24		2.78		3–4	67	Kilada et al. 2007
	21B	Sable Bank	33	1964	52.5		105.43		2.38		3–4	–119	Kilada et al. 2007
	21C	Sable Bank	33	1976.5	76.2		107.97		1.42		3–4	319	Kilada et al. 2007
	11A	Sable Bank	37	1957	27.7		102.86		2.38		3–4	–616	Kilada et al. 2007
	11B	Sable Bank	37	1968	90.7		109.31		2.19		3–4	94	Kilada et al. 2007
	11C	Sable Bank	37	1981	70.9		107.49		1.72		3–4	288	Kilada et al. 2007
	15A	Sable Bank	37	1956	–69.3		93.14		2.85		3–4	145	Kilada et al. 2007
	15B	Sable Bank	37	1969.5	66.4		106.89		2.15		3–4	338	Kilada et al. 2007
	15C	Sable Bank	37	1978.5	78.4		108.21		1.69		3–4	275	Kilada et al. 2007
Mixed-layer modeled data			0–75	1950	–55.5		94.45					0	Reimer et al. 2009

Table 2 ^{14}C data, laboratory codes, sample identification codes, and references. The ΔR values before and during the bomb pulse are calculated as the difference between the measured ^{14}C age (= 8033 ln(pMC/100)) and the age expected from the Marine09 calibration curve or the post-bomb modeled marine response (given at the end of the table (Reimer et al. 2009), respectively. The ΔR calculations are based on a moving average of the marine model data corresponding to the number of years integrated in each sample. The 1950 reference value is taken as the average of the 2 curves (* = estimated value; ΔR = ^{14}C age–Marine09). *(Continued)*

Lab code	Sample ID	Site	Depth (m)	Year (AD)	$\Delta^{14}C$	Error (±1σ)	pMC	Error (±1σ)	$\delta^{13}C$	Error (±1σ)	SI yr[a]	ΔR	Reference
Mixed-layer modeled data			0–75	1951	–55.8		94.43					0	Reimer et al. 2009
Mixed-layer modeled data			0–75	1952	–56.0		94.42					0	Reimer et al. 2009
Mixed-layer modeled data			0–75	1953	–56.2		94.41					0	Reimer et al. 2009
Mixed-layer modeled data			0–75	1954	–56.2		94.42					0	Reimer et al. 2009
Mixed-layer modeled data			0–75	1955	–55.2		94.54					0	Reimer et al. 2009
Mixed-layer modeled data			0–75	1956	–52.6		94.81					0	Reimer et al. 2009
Mixed-layer modeled data			0–75	1957	–49.1		95.17					0	Reimer et al. 2009
Mixed-layer modeled data			0–75	1958	–42.9		95.81					0	Reimer et al. 2009
Mixed-layer modeled data			0–75	1959	–34.5		96.65					0	Reimer et al. 2009
Mixed-layer modeled data			0–75	1960	–26.1		97.51					0	Reimer et al. 2009
Mixed-layer modeled data			0–75	1961	–18.8		98.25					0	Reimer et al. 2009
Mixed-layer modeled data			0–75	1962	–9.7		99.17					0	Reimer et al. 2009
Mixed-layer modeled data			0–75	1963	8.2		100.98					0	Reimer et al. 2009
Mixed-layer modeled data			0–75	1964	38.1		103.99					0	Reimer et al. 2009
Mixed-layer modeled data			0–75	1965	65.4		106.74					0	Reimer et al. 2009
Mixed-layer modeled data			0–75	1966	84.0		108.61					0	Reimer et al. 2009
Mixed-layer modeled data			0–75	1967	96.0		109.83					0	Reimer et al. 2009
Mixed-layer modeled data			0–75	1968	104.3		110.67					0	Reimer et al. 2009
Mixed-layer modeled data			0–75	1969	110.3		111.29					0	Reimer et al. 2009
Mixed-layer modeled data			0–75	1970	115.2		111.79					0	Reimer et al. 2009
Mixed-layer modeled data			0–75	1971	119.3		112.21					0	Reimer et al. 2009
Mixed-layer modeled data			0–75	1972	121.9		112.49					0	Reimer et al. 2009
Mixed-layer modeled data			0–75	1973	123.2		112.63					0	Reimer et al. 2009
Mixed-layer modeled data			0–75	1974	123.2		112.65					0	Reimer et al. 2009
Mixed-layer modeled data			0–75	1975	122.5		112.59					0	Reimer et al. 2009
Mixed-layer modeled data			0–75	1976	121.1		112.46					0	Reimer et al. 2009
Mixed-layer modeled data			0–75	1977	118.9		112.25					0	Reimer et al. 2009
Mixed-layer modeled data			0–75	1978	117.0		112.08					0	Reimer et al. 2009
Mixed-layer modeled data			0–75	1979	115.2		111.91					0	Reimer et al. 2009
Mixed-layer modeled data			0–75	1980	112.8		111.69					0	Reimer et al. 2009
Mixed-layer modeled data			0–75	1981	110.0		111.42					0	Reimer et al. 2009

Table 2 ^{14}C data, laboratory codes, sample identification codes, and references. The ΔR values before and during the bomb pulse are calculated as the difference between the measured ^{14}C age (= 8033 ln(pMC/100)) and the age expected from the Marine09 calibration curve or the post-bomb modeled marine response (given at the end of the table (Reimer et al. 2009), respectively. The ΔR calculations are based on a moving average of the marine model data corresponding to the number of years integrated in each sample. The 1950 reference value is taken as the average of the 2 curves (* = estimated value; ΔR = ^{14}C age–Marine09). *(Continued)*

Lab code	Sample ID	Site	Depth (m)	Year (AD)	$\Delta^{14}C$	Error (±1σ)	pMC	Error (±1σ)	$\delta^{13}C$	Error (±1σ)	SI yr[a]	ΔR	Reference
Mixed-layer modeled data			0–75	1982	106.9		111.12					0	Reimer et al. 2009
Mixed-layer modeled data			0–75	1983	103.9		110.84					0	Reimer et al. 2009
Mixed-layer modeled data			0–75	1984	100.9		110.55					0	Reimer et al. 2009
Mixed-layer modeled data			0–75	1985	97.8		110.25					0	Reimer et al. 2009
Mixed-layer modeled data			0–75	1986	94.7		109.95					0	Reimer et al. 2009
Mixed-layer modeled data			0–75	1987	91.7		109.66					0	Reimer et al. 2009
Mixed-layer modeled data			0–75	1988	88.6		109.36					0	Reimer et al. 2009
Mixed-layer modeled data			0–75	1989	85.6		109.08					0	Reimer et al. 2009
Mixed-layer modeled data			0–75	1990	82.7		108.79					0	Reimer et al. 2009
Mixed-layer modeled data			0–75	1991	79.8		108.51					0	Reimer et al. 2009
Mixed-layer modeled data			0–75	1992	76.7		108.22					0	Reimer et al. 2009
Mixed-layer modeled data			0–75	1993	73.8		107.94					0	Reimer et al. 2009
Mixed-layer modeled data			0–75	1994	70.8		107.65					0	Reimer et al. 2009
Mixed-layer modeled data			0–75	1995	67.9		107.38					0	Reimer et al. 2009
Mixed-layer modeled data			0–75	1996	65.2		107.11					0	Reimer et al. 2009

[a]SI yr = sample integration years.

There is therefore a clear gradient of increasing amplitude of the bomb pulse from the north Icelandic shelf, Georges and Sable banks, Tromsø through to the North Sea (Figure 3). This gradient is also matched in the timing of the peak $\Delta^{14}C$ values: the peak is earliest in the German Bight (1967) and in the Oyster Ground (1966) and most recent on the north Icelandic shelf (up to 1980). Apart from Sable Bank, all sites show an initial and rapid response around 1958 within a year of the start of the atmospheric $\Delta^{14}C$ excess; Sable Bank contains a single data point with an early rise to 103 pMC in 1957. The atmospheric peak was reached very rapidly, by 1963, after a small reversal in 1960–1962 resulting from the 1958–1962 moratorium on weapons testing imposed by the Geneva Convention, and declined rapidly after reaching this peak. The peak in all marine inventories is therefore delayed with respect to the atmospheric peak. The marine series, however, all remain high and plateau for a significant period while atmospheric values rapidly decline (Figure 3). This slow relaxation is also phased between the sites; significant reduction in $\Delta^{14}C$ excess is recorded in the North Sea around 1975, in Tromsø around 1976–77, at Siglufjordur (north Icelandic shelf) around 1980, and at Grimsey (north Icelandic shelf) not until 2000. The resolution of the Georges (Weidman and Jones 1993) and Sable bank (Kilada et al. 2007) series are not sufficient to identify with any certainty the timing of the marked decline in excess. There is a clear reversal in the rising limb of the Sable Bank data, and an inflection in the Grimsey (north Icelandic shelf) series, but these changes predate the timing in the reduction in the rate of the rise of atmospheric bomb pulse; for the Grimsey series, this cannot result from an error in the chronology since this series has been cross-dated (Butler et al. 2012). The inflection in the rising limb of the German Bight series between 1960 and 1962 is, however, consistent with the timing in the reduction in the rate of the rise of atmospheric $\Delta^{14}C$.

DISCUSSION

Hydrographic Context of the Sites

The global modeled marine curve is damped with respect to the atmospheric signal because of the relative size of the marine and atmospheric carbon reservoirs (Figure 3). The key variables determining the character of the marine bomb pulse in any particular coastal or shelf region are both physical and biogeochemical. Physical controls include the age (extent of depletion) of the precursor marine water masses and rates of vertical mixing, rates of air-sea CO_2 exchange, the ^{14}C content of inflowing freshwater, and the depth and rate of exchange between coastal basins and the open ocean. Biogeochemical controls are dominated by the rates of primary production, the flux of organic carbon to the seabed, and the residence time of organic matter within the sediment mixed layer; these factors together control the availability of organic matter containing variable excess ^{14}C as a carbon source for *A. islandica*. The percentage of metabolic carbon uptake in *A. islandica* is consistent across growth rates and ages, and is always below 10% (Beirne et al. 2012).

In the pre-bomb era, marine sites influenced by ^{14}C-enriched waters as a result of enhanced exchange with the atmosphere in restricted basins or significant freshwater input show significantly reduced local reservoir ages (negative ΔR) and marine sites influenced by upwelling of ^{14}C-depleted deep, old water (e.g. Antarctica, coastal Peru, north Icelandic shelf) show high local reservoir ages ($\Delta R >> 0$). The overall magnitude and the temporal offsets between the maximum peaks in the post-bomb atmospheric and marine curves result from the mixing of deep water with water recently ventilated by air at the sea surface containing elevated levels of ^{14}C through atmospheric testing of atomic weapons. The damped and strongly attenuated records are therefore from sites characterized by pre-bomb ΔR values greater than 0, such as the north Icelandic shelf. Here, immediately pre-bomb ΔR values (AD 1650 to 1950) have been constrained to between +100 and +400 based on

measurement of both pre-bomb *A. islandica* increments and tephra age-model-constrained foraminifera and mollusks (Eiríksson et al. 2004; Wanamaker et al. 2008). The data presented here for the 1940 and 1950 increments from the Grimsey series are $\Delta R = +120$ (pMC = 93.03) and +95 (pMC = 93.28), respectively (Table 2; Figure 3). In the German Bight, however, pre-bomb ΔR values reach as low as –53 (Figure 3; Table 2). This contrast can be at least partially attributed to the entrainment of old, deep waters on the north Icelandic shelf, notably modified Arctic water of the East Icelandic and East Greenland currents (Eiríksson et al. 2004; Wanamaker et al. 2008), in comparison to the German Bight, which is far removed from the influence of upwelled deep-water masses and characterized by restricted exchange.

Rates of air-sea CO_2 exchange in shelf seas are a function of physical controls, largely wind and sea surface temperature, and biological controls, principally the balance between production and respiration (Thomas et al. 2004). Assimilation of atmospheric ^{14}C excess will be rapid in shallow basins with restricted exchange (Heier-Nielsen et al. 1995); this is the "shelf sea effect." Permanently mixed areas, such as the German Bight, tend to be weak CO_2 sources, whereas seasonally stratified areas, such as the northern North Sea, are CO_2 sinks, constituting the continental shelf pump component of the ocean biological pump (Rippeth et al. 2008). Rapid exchange of CO_2 between air and river water sources (soil moisture) results in freshwater $\Delta^{14}C$ excess close to equilibrium with the atmosphere unless there is inert bedrock or old carbon, notably soil carbon, sources accessed within the catchment, or if the water sources have a long residence time.

Freshwater can have very variable ^{14}C content, ranging from settings with significant lake-related reservoir ages and hardwater effects (cf. Heier-Nielsen et al. 1995) to enriched inflow resulting from rapid exchange with the atmosphere with zero ^{14}C reservoir age. For any basin experiencing steady-state carbon exchange with the atmosphere, the reservoir age will be seen to increase with the increasing size of the marine to atmosphere reservoir ratio; hence, shallow basins with large surface area and restricted exchange with the open ocean will have low reservoir age (Heier-Nielsen et al. 1995).

The near-instantaneous response of the marine $\Delta^{14}C$ excess records to the start of the atmospheric increase can be attributed to the importance of air-sea exchange. The reduced magnitude, delayed response, and attenuated decline of the bomb pulse in the ocean reflects the time required for isotopic equilibration, which is slower than CO_2 equilibration (Lynch-Stieglitz et al. 1995), resulting from air-sea isotopic exchange and mixing with the larger carbon reservoir in the mixed layer. Therefore, sites with low ΔR values, such as the German Bight, characterized by small carbon reservoirs in the mixed layer, might be expected to reach a peak more quickly through air-sea exchange than sites strongly influenced by mixing with larger reservoirs, such as the north Icelandic shelf. As might be expected from their strongly positive ΔR values, the most strongly attenuated of the *A. islandica* bomb-pulse series are indeed from the north Icelandic shelf; these are coastal sites with open exchange with deep, old water masses. The Siglufjordur specimen (pMC peak of 105.7 at 1971) was from 20 m, close to the coast, and Grimsey (peak 104.3, 1985) at 80 m on the open shelf; the small offset in the timing and magnitude of $\Delta^{14}C$ excess between the 2 sites can probably be attributed to the shelf sea effect given the difference in water depths between the 2 sites. It is unlikely that freshwater input is significant since both north Icelandic shelf sites are close to normal fully marine salinities; Siglufjordur has a smaller drainage basin than most fjords in north Iceland, receiving little water from central Iceland or glacial meltwater. The Georges and Sable bank series are also quite attenuated and these data highlight the significance of depleted Labrador Sea water in influencing the character of the $\Delta^{14}C$ record along this margin (Weidman and Jones 1993). The Tromsø record is from a very shallow site influenced by waters with ΔR values close to the global modeled mean (North Atlantic Current) and rapid assimilation of the atmospheric bomb pulse is to be expected in such a setting.

The inflections in the rate of increase in $\Delta^{14}C$ in the German Bight and Grimsey (north Icelandic shelf) series are within the range of natural variability in the pre-bomb era, as demonstrated by the Oyster Ground series (Figure 3; Witbaard et al. 1994). Even though the German Bight inflection in the 1960–1962 period is coincident with, but an attenuated form of, the actual decline in atmospheric $\Delta^{14}C$ excess resulting from the moratorium on atmospheric weapons testing, it may therefore not be a reflection of air-sea exchange and rapid assimilation of the atmospheric signal. Grimsey and Siglufjordur lack the early upward inflection that characterizes the other sites possibly because they are generally more attenuated than the other sites. There is no detectable plateau or reduction in ^{14}C excess associated with the GSA (Figure 4).

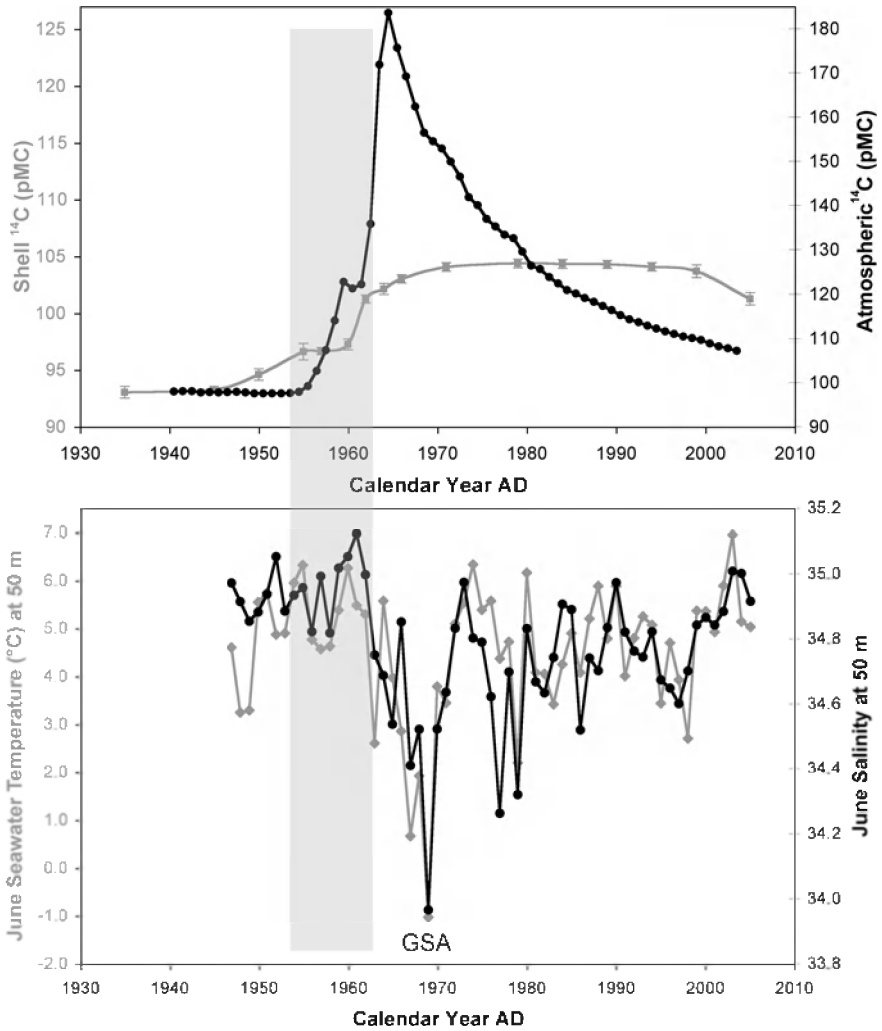

Figure 4 Detail of north Icelandic sites (lower amplitude) with atmospheric bomb pulse (upper panel). Lower panel shows summer temperature and salinity data at 50 m are from Iceland (Grimsey) from the Marine Research Institute Reykjavík, Iceland (http://www.hafro.is/Sjora/). It is clear that the inflection in the Grimsey bomb pulse is synchronous with the atmospheric bomb pulse and does not relate to the later Great Salinity Anomaly (GSA).

The rapid response of the shallow North Sea settings might be related to the high primary production rates in the area (Joint and Pomroy 1993). This high productivity causes a rapid transport of organic material to the seafloor and rapid incorporation into the ecosystem. In some settings, including the Oyster Ground, some of this material is buried up to 20 cm into the sediments and this might function as a long-term source of excess ^{14}C. This might therefore explain the long attenuation time for the shallow marine sites in high-productivity areas after the decline of the atmospheric peak.

A number of annually resolved $\delta^{13}C$ records are now available from *A. islandica* growth increments from sites across the North Atlantic, all of which show a distinct negative shift in $\delta^{13}C$ since ~AD 1900 (Butler et al. 2009; Schöne et al. 2011). This has been attributed to the oceanic Suess effect arising from the incorporation of isotopically light anthropogenic CO_2 into the surface ocean. Both the Suess effect and the bomb pulse result from the anthropogenic emission of isotopically distinctive carbon, but at different times; the 2 events also differ in that the Suess effect has increased exponentially since inception, whereas the bomb pulse was a sharp peak followed by rapid decline. As the physical and biogeochemical processes controlling the incorporation of anthropogenic CO_2 into the ocean will be the same as those controlling the incorporation of the ^{14}C bomb pulse, we hypothesize that the regional differences in the expression of the oceanic Suess effect (absolute values, attenuation, rate of uptake) measured from known-age marine bivalve increments will positively correlate with the regional differences in $\Delta^{14}C$, i.e. the damped and attenuated bomb-pulse records will have a similar expression for the inception of the Suess effect, and the offsets between sites will be a function of the isotopic composition of the water masses concerned.

Applications

In order to constrain the rates of natural and anthropogenically forced processes in the marine environment, it is critical that robust geochronological techniques are available. This is particularly the case for the past 6 decades, which cover a significant proportion of the industrial period most impacted by anthropogenic influence and in which the detection of systems changes forced by anthropogenic versus naturally occurring processes is critical. Key applications that require such recent dating control include 1) vertical mixing and diffusion of materials, notably contaminants, by bioturbation and physical processes within the sediment mixed layer; 2) calculation of sedimentation rates and influx data (concentration × sedimentation rate) for key sediment components (e.g. microfossil groups, lithic particles including ice-rafted detritus); 3) carbon-cycle processes across and within the benthic boundary layer; 4) range extensions of marine organisms forced by seawater temperature change; 5) decadal-scale reconstructions of coastal water mass origins and mixing; and 6) the timing of marine climatic changes over the past century.

Typically, sedimentation rates from cores of surficial sediments (box, multi-, gravity cores) are constructed using AMS ^{14}C before ~250 yr BP, followed by ^{210}Pb and/or ^{137}Cs or other event markers (e.g. Pb isotopes, tephra) for the last few decades. In many cases, however, the "splicing" of chronologies based on different methods is problematic, resulting in reconstructed jumps in sedimentation rates that are intuitively unlikely (cf. Lebreiro et al. 2006). Similarly, the interpretation of ^{137}Cs peaks based on atmospheric fallout event histories can be difficult, as can the interpretation of ^{210}Pb data via constant rate-of-supply (CRS) modeling (Appleby 2001). The $\Delta^{14}C$ excess inventories presented here provide the basis for calibration of post-bomb AMS ^{14}C determinations from surficial marine sediments (using typically foraminifera or mollusks as the dated material) from the regions investigated without recourse to additional techniques or approaches. In some cases, single probability peak solutions may be possible, but in most cases, because of the overall form of the bomb-pulse curve and its double-peaked character, at least 2 potential high-probability solutions

may be possible. If short-lived bivalve mollusks are being used as the dated medium, this problem can be circumvented by dating both the start and the end of growth series to assess whether the rising (low→high pMC), or the falling (high→low pMC), limb of the curve presents the highest probability solution. The strong regional differences identified, however, indicate that care should be taken to assess the hydrographic similarity of any individual *A. islandica* "calibration curve" to the setting of the sequence to be calibrated. It would clearly not be appropriate, for instance, to calibrate ^{14}C determinations from a sediment sequence in the German Bight with a curve from the north Icelandic shelf.

Dynamical oceanographic investigations of mixing in coastal and shelf waters are usually limited to the timeframe of the duration of individual experiments, typically only a few years (cf. Simpson 1993). The marine bomb-pulse ^{14}C data presented here provide data for validation of the hydrodynamic modeling of mixing processes in the coastal ocean over the 10–100 yr timescale. The data also constitute a key baseline for the management of coastal systems in the context of contaminant releases, some of which may involve radionuclides with long half-lives, the radiation from which will impact the marine system for significant periods of time.

Research into species' distribution changes (range extensions) and ecosystem functioning in relation to recent climate change and anthropogenic dispersals is restricted to analysis of data from long-term monitoring programs (Hawkins et al. 2003) in the absence of access to high-resolution geochronology. The $\Delta^{14}C$ excess series presented here provide a basis for the dating of dead but unstratified preserved materials (shell/valve carbonate, teeth, otolith, statolith, bone), for instance from subtidal lags, and from intertidal accumulations, at high precision. This will enable range extension rates to be established for species for which data are not currently available from long-term monitoring, and will permit detailed statistical analysis of such changes with instrumental (temperature, salinity, nutrients) data sets. The series will also provide critical information for studies in marine ecology, such as evaluating the age of fish populations (e.g. Campana and Jones 1998; Kerr et al. 2005), identifying the environmental agents implicated in the decline of maerl (coralline algal) beds (e.g. Blake et al. 2007) and the characterization of particulate organic matter in coastal waters (e.g. Megens et al. 2001).

Given the demonstrated within-region variability of the signature of the marine bomb pulse exemplified by the north Icelandic shelf and North Sea data pairs (Figure 3), for dating exercises of this kind it is recommended that multiple rather than single series are used to generate calibration data sets.

CONCLUSIONS

1. Measurement of $\Delta^{14}C$ excess from known-age annual increments of the long-lived bivalve mollusk *Arctica islandica* from 7 sites across the coastal North Atlantic demonstrates strong regional variability in the character of the marine bomb pulse.
2. This variability can be attributed to differences in the hydrographic and biogeochemical setting of the sites relating to entrainment of old, deep, upwelled water masses; processes controlling the isotopic exchange of ^{14}C at the air-sea boundary; salinity as a function of the flux of freshwater into the coastal ocean; and the productivity and flux to, and the residence time of organic matter within, the sediment mixed layer.
3. The inventories form a sequence from high magnitude-early peak to low magnitude-late peak, in the following order of increasing attenuation: German Bight (southern North Sea), Oyster Ground (southern North Sea), Tromsø, Sable Bank, Georges Bank, Siglufjorder (north Icelandic coast), Grimsey (north Icelandic shelf).

4. All series show a rapid response to the increase in atmospheric $\Delta^{14}C$ excess but a slow response to the subsequent decline resulting from a combination of rapid isotopic air-sea exchange, continued entrainment of older water masses, and incorporation of buried organic matter.
5. Given the resolution of the data, there is no statistically significant inflection in the rate of rise, or reversal, in marine $\Delta^{14}C$ excess coincident with the temporary reversal in the rise of atmospheric $\Delta^{14}C$ excess resulting from the 1958–1962 moratorium on atmospheric nuclear weapons testing.
6. The Great Salinity Anomaly of the late 1960s on the north Icelandic shelf, associated with the advection of the "old" East Icelandic Current linked to the southward migration of the Polar Front, did not impact on the character of the north Icelandic bomb-pulse records.
7. The inventories constitute calibration series for the use of the bomb pulse as a high-resolution dating tool in the marine environment. Applications include 1) vertical mixing and diffusion of materials, notably contaminants, by bioturbation and physical processes within the sediment mixed layer; 2) calculation of sedimentation rates and influx data (concentration × sedimentation rate) for key sediment components (e.g. microfossil groups, lithic particles including ice-rafted detritus); 3) carbon-cycle processes across and within the benthic boundary layer; 4) range extensions of marine organisms forced by seawater temperature change; 5) decadal-scale reconstructions of coastal water mass origins and mixing; and 6) the timing of marine climatic changes over the past century.

The atmospheric bomb pulse therefore constitutes a step-function whose response in the marine environment is immediate but of smaller amplitude and with a longer decay time as a function of the much larger reservoir; the character of this attenuation is a function of regional hydrography and biogeochemistry.

ACKNOWLEDGMENTS

The Grimsey measurements and paper compilation were undertaken as part of the EU Framework 6 MILLENNIUM Integrated Project (SUSTDEV-2004-3.1.4.1, 017008-2) "European climate of the last millennium." JDS acknowledges support from a Royal Society-Leverhulme Trust Senior Research Fellowship. This paper is a contribution to the Climate Change Consortium of Wales (C3W). The constructive comments of 2 anonymous referees are acknowledged.

REFERENCES

Andersen GJ, Heinemeier J, Nielsen HL, Rud N, Thomsen MS, Johnsen S, Sveinbjörnsdóttir A, Hjartarson Á. 1989. AMS ^{14}C dating on the Fossvogur sediments, Iceland. *Radiocarbon* 31(3):592–600.

Appleby PG. 2001. Chronostratigraphic techniques in recent sediments. In: Last WM, Smol JP, editors. *Tracking Environmental Change Using Lake Sediments. Volume 1: Basin Analysis, Coring and Chronological Techniques*. Berlin: Springer-Verlag. p 171–203.

Ardizzone D, Cailliet GM, Natanson LJ, Andrews AH, Kerr LA, Brown TA. 2006. Application of bomb radiocarbon chronologies to shortfin mako (*Isurus oxyrinchus*) age validation. *Environmental Biology of Fishes* 77(3–4):355–66.

Beirne EC, Wanamaker Jr AD, Feindel SC. 2012. Experimental validation of environmental controls on the $\delta^{13}C$ of *Arctica islandica* (ocean quahog) shell carbonate. *Geochimica et Cosmochimica Acta* 84:395–409.

Blake C, Maggs C, Reimer PJ. 2007. Use of radiocarbon dating to interpret past environments of maerl beds. *Ciencias Marinas* 33(4):385–97.

Broecker WS, Peng TH. 1982. *Tracers in the Sea*. New York: Lamont-Doherty Earth Observatory, Columbia University.

Broecker WS, Peng TH, Takahashi T. 1980. A strategy for the use of bomb-produced radiocarbon as a tracer for the transport of fossil fuel CO_2 into the deep-sea source regions. *Earth and Planetary Science Letters* 49(2):463–8.

Butler PG, Scourse JD, Richardson CA, Wanamaker Jr AD, Bryant CL, Bennell JD. 2009. Continuous marine radiocarbon reservoir calibration and the ^{13}C Suess effect in the Irish Sea: results from the first multi-centennial shell-based marine master chronology. *Earth and Planetary Science Letters* 279(3–4):230–41.

Butler PG, Wanamaker Jr AD, Scourse JD, Richardson

CA, Reynolds DJ. 2012. Variability of marine climate on the North Icelandic Shelf in a 1357-year proxy archive based on growth increments in the bivalve *Arctica islandica*. *Palaeogeography, Palaeoclimatology, Palaeoecology*: doi:10.1016/j.palaeo.2012.01.016.

Campana SE, Jones CM. 1998. Radiocarbon from nuclear testing applied to age validation of black drum, *Pogonias cromis*. *Fishery Bulletin* 96(2):185–92.

Campana SE, Casselman JM, Jones CM. 2008. Bomb radiocarbon chronologies in the Arctic, with implications for the age validation of lake trout (*Salvelinus namaycush*) and other Arctic species. *Canadian Journal of Fisheries and Aquatic Sciences* 65(4):733–43.

Chapman DC, Beardsley RC. 1989. On the origin of shelf water in the Middle Atlantic Bight. *Journal of Physical Oceanography* 19(3):384–91.

Dahlgren TG, Weinberg JR, Halanych KM. 2000. Phylogeography of the ocean quahog (*Arctica islandica*): influences of paleoclimate on genetic diversity and species range. *Marine Biology* 137(3):487–95.

Dickson RR, Meincke J, Malmberg SA, Lee AJ. 1988. The 'Great Salinity Anomaly' in the northern North Atlantic 1968–1982. *Progress in Oceanography* 20(2):103–51.

Druffel ERM. 1987. Bomb radiocarbon in the Pacific: annual and seasonal time scale variations. *Journal of Marine Research* 45(3):667–98.

Druffel ERM. 1989. Decade time scale variability of ventilation in the North Atlantic: high-precision measurements of bomb radiocarbon in banded corals. *Journal of Geophysical Research* 94(C3):3271–85.

Druffel ERM 1997. Pulses of rapid ventilation in the North Atlantic surface ocean during the past century. *Science* 275(5305): 1454–7.

Druffel ERM, Robinson LF, Griffin S, Halley RB, Southon JR, Adkins JF. 2008. Low reservoir ages for the surface ocean from mid-Holocene Florida corals. *Paleoceanography* 23(2):PA2209, doi:10.1029/2007PA001527.

Eiríksson J, Larsen G, Knudsen KL, Heinemeier J, Simonarson LA. 2004. Marine reservoir age variability and water mass distribution in the Iceland Sea. *Quaternary Science Reviews* 23(20–22):2247–68.

Eiríksson J, Knudsen KL, Larsen G, Olsen J, Heinemeier J, Bartels-Jónsdóttir HB, Jiang H, Ran L, Símonarson LA. 2011. Coupling of palaeoceanographic shifts and changes in marine reservoir ages off North Iceland through the last millennium. *Palaeogeography, Palaeoclimatology, Palaeoecology* 302(1–2):95–108.

Gagnon AR, Jones GA. 1993. AMS-graphite target production methods at the Woods Hole Oceanographic Institution between 1986–91. *Radiocarbon* 35(2): 301–10.

Goodsite ME, Rom W, Heinemeier J, Lange T, Ooi S, Appleby PG, Shotyk W, van der Knapp WO, Lohse C, Hansen TS. 2001. High-resolution AMS ^{14}C dating of post-bomb peat archives of atmospheric pollutants. *Radiocarbon* 43(2B):495–515.

Gruber N. 1998. Anthropogenic CO_2 in the Atlantic Ocean. *Global Biogeochemical Cycles* 12(1):165–91.

Grumet NS, Guilderson TP, Dunbar RB. 2002. Meridional transport in the Indian Ocean traced by coral radiocarbon. *Journal of Marine Research* 60(5):725–42.

Guilderson TP, Schrag DP. 1998. Abrupt shift in subsurface temperatures in the eastern tropical Pacific associated with recent changes in El Niño. *Science* 281(5374):241–3.

Guilderson TP, Schrag DP, Kashgarian M, Southon J. 1998. Radiocarbon variability in the Western Equatorial Pacific inferred from a high-resolution coral record from Nauru Island. *Journal of Geophysical Research* 103(C11):24,641–50.

Guilderson TP, Schrag DP, Goddard E, Kashgarian M, Wellington GM, Linsley BK. 2000. Southwest subtropical Pacific surface water radiocarbon in a high-resolution coral record. *Radiocarbon* 42(2):249–56.

Hannah CG, Shore JA, Loder JW, Naimie CE. 2001. Seasonal circulation on the Western and Central Scotian Shelf. *Journal of Physical Oceanography* 31(2):591–615.

Hardisty J. 1990. *The British Seas*. London: Routledge.

Hawkins SJ, Southward AJ, Genner MJ. 2003. Detection of environmental change in a marine ecosystem – evidence from the western English Channel. *Science of the Total Environment* 310(1–3):245–56.

Heier-Nielsen S, Heinemeier J, Nielsen HL, Rud N. 1995. Recent reservoir ages for Danish fjords and marine waters. *Radiocarbon* 37(2):875–82.

Hill AE, James ID, Linden PF, Matthews JP, Prandle D, Simpson JH, Gmitrowicz EM, Smeed DA, Lwiza KMM, Durazo R, Fox AD, Bowers DG. 1993. Dynamics of tidal mixing fronts in the North Sea. *Philosophical Transactions of the Royal Society of London A* 343(1669):431–46.

Hua Q, Woodroffe CD, Smithers SG, Barbetti M, Fink D. 2005. Radiocarbon in corals from the Cocos (Keeling) Islands and implications for Indian Ocean circulation. *Geophysical Research Letters* 32(21):L21602, doi: 10.1029/2005GL023882.

Johannessen OM. 1986. Brief overview of the physical oceanography. In: Hurdle BG, editor. *The Nordic Seas*. New York: Springer-Verlag. p 103–27

Joint I, Pomroy A. 1993. Phytoplankton biomass and production in the southern North Sea. *Marine Ecology Progress Series* 99(1–2):169–82.

Jones DS. 1983. Sclerochronology – reading the record of the molluscan shell. *American Scientist* 71(4):384–91.

Kalish JM, Nydal R, Nedreaas KH, Burr GS, Eine GL. 2001. A time history of pre- and post-bomb radiocarbon in the Barents Sea derived from Arcto-Norwegian cod otoliths. *Radiocarbon* 43(2):843–55.

Kerr LA, Andrews AH, Munk K, Coale KH, Frantz BR, Caillet GM, Brown TA. 2005. Age validation of quillback rockfish (*Sebastes maliger*) using bomb radiocarbon. *Fishery Bulletin* 103(1):97–107.

Kilada RW, Campana SE, Roddick D. 2007. Validated age, growth, and mortality estimates of the ocean quahog (*Arctica islandica*) in the western Atlantic. *ICES Journal of Marine Science* 64(1):31–8.

Kilada RW, Campana SE, Roddick D. 2009. Growth and sexual maturity of the northern propellorclam (*Cyrtodaria siliqua*) in Eastern Canada, with bomb radiocarbon age validation. *Marine Biology* 156(5):1029–37.

Kilbourne KH, Quinn TM, Guilderson TP, Webb RS, Taylor FW. 2007. Decadal- to interannual-scale source water variations in the Caribbean Sea recorded by Puerto Rican coral radiocarbon. *Climate Dynamics* 29(1):51–62.

Knudsen KL, Eiríksson J. 2002. Application of tephrochronology to the timing and correlation of palaeoceanographic events recorded in Holocene and Late Glacial shelf sediments off North Iceland. *Marine Geology* 191(3–4):165–88.

Knudsen KL, Eiríksson J, Jansen E, Jiang H, Rytter F, Gudmundsdóttir ER. 2004. Palaeoceanographic changes off North Iceland through the last 1200 years: foraminifera, stable isotopes, diatoms and ice rafted debris. *Quaternary Science Reviews* 23(20–22):2231–46.

Lebreiro SM, Francés G, Abrantes FFG, Diz P, Bartels-Jónsdóttir HB, Stroynowski Z, Gil IM, Pena L, Rodrigues T, Jones PD, Nombela MA, Alejo I, Briffa KR, Harris I, Grimalt JO. 2006. Climate change and coastal hydrographic response along the Atlantic Iberian margin (Tagus Prodelta and Muros Ría) during the last two millennia. *The Holocene* 16(7):1003–15.

Levin I, Kromer B. 2004. The tropospheric $^{14}CO_2$ level in mid-latitudes of the Northern Hemisphere (1959–2003). *Radiocarbon* 46(3):1261–72.

Levin I, Hammer S, Kromer B, Meinhardt F. 2008. Radiocarbon observations in atmospheric CO_2: determining fossil fuel CO_2 over Europe using Jungfraujoch observations as background. *Science of the Total Environment* 391(2–3):211–6.

Lynch-Stieglitz J, Stocker TF, Broecker WS, Fairbanks RG. 1995. The influence of air-sea exchange on the isotopic composition of oceanic carbon – observations and modelling. *Global Biogechemical Cycles* 9(4): 653–65.

Mahadevan A. 2001. An analysis of bomb radiocarbon trends in the Pacific. *Marine Chemistry* 73(3–4):273–90.

Megens L, van der Plicht J, de Leeuw JW. 2001. Temporal variations in ^{13}C and ^{14}C concentrations in particulate organic matter from the southern North Sea *Geochimica et Cosmochimica Acta* 65(17):2899–911.

Müller SA, Joos F, Plattner GK, Edwards NR, Stocker TF. 2008. Modeled natural and excess radiocarbon: sensitivities to the gas exchange formulation and ocean transport strength. *Global Biogeochemical Cycles* 22(3):GB3011, doi:10.1029/2007GB003065.

Murawski SA, Ropes JW, Serchuk FM. 1982. Growth of the ocean quahog, *Arctica islandica*, in the Middle Atlantic Bight. *Fishery Bulletin* 80(1):21–43.

Ohkouchi N, Eglinton TI, Hayes JM. 2003. Radiocarbon dating of individual fatty acids as a tool for refining Antarctic margin sediment chronologies. *Radiocarbon* 45(1):17–24.

Ólafsson J. 1999. Connections between oceanic conditions off N. Iceland, Lake Mývatn temperature, regional wind direction variability and the North Atlantic Oscillation. *Rit Fiskideildar* 16:41–57.

Reimer PJ, Baillie MGL, Bard E, Bayliss A, Beck JW, Bertrand CJH, Blackwell PG, Buck CE, Burr GS, Cutler KB, Damon PE, Edwards RL, Fairbanks RG, Friedrich M, Guilderson TP, Hogg AG, Hughen KA, Kromer B, McCormac G, Manning S, Bronk Ramsey C, Reimer RW, Remmele S, Southon JR, Stuiver M, Talamo S, Taylor FW, van der Plicht J, Weyhenmeyer CE. 2004. IntCal04 terrestrial radiocarbon age calibration, 0–26 cal kyr BP. *Radiocarbon* 46(3):1029–58.

Reimer PJ, Baillie MGL, Bard E, Bayliss A, Beck JW, Blackwell PG, Bronk Ramsey C, Buck CE, Burr GS, Edwards RL, Friedrich M, Grootes PM, Guilderson TP, Hajdas I, Heaton TJ, Hogg AG, Hughen KA, Kaiser KF, Kromer B, McCormac FG, Manning SW, Reimer RW, Richards DA, Southon JR, Talamo S, Turney CSM, van der Plicht J, Weyhenmeyer CE. 2009. IntCal09 and Marine09 radiocarbon age calibration curves, 0–50,000 years cal BP. *Radiocarbon* 51(4): 1111–50.

Rippeth TP, Scourse JD, Uehara K, McKeown S. 2008. The impact of sea-level rise over the last deglacial transition on the strength of the continental shelf CO_2 pump. *Geophysical Research Letters* 35(24):L24604, doi:10.1029/2008GL035880.

Ropes JW. 1984. Procedures for preparing acetate peels and evidence validating the annual periodicity of growth lines formed in the shells of ocean quahogs, *Arctica islandica*. *Marine Fisheries Review* 46(2):27–35.

Rytter F, Knudsen KL, Seidenkrantz M-S, Eiríksson J. 2002. Modern distribution of benthic foraminifera on the North Icelandic shelf and slope. *Journal of Foraminiferal Research* 32(3):217–44.

Schöne BR, Houk SD, Castro ADF, Fiebig J, Oschmann W, Krönke I, Dreyer W, Gosselck F. 2005. Daily growth rates in shells of *Arctica islandica*: assessing sub-seasonal environmental controls on a long-lived bivalve mollusc. *Palaios* 20(1):78–92.

Schöne BR, Wanamaker Jr AD, Fiebig J, Thébault J, Kreutz K. 2011. Annually resolved $\delta^{13}C$ shell chronologies of long-lived bivalve mollusks (*Arctica islandica*) reveal oceanic carbon dynamics in the temperate North Atlantic during recent centuries. *Palaeogeography, Palaeoclimatology, Palaeoecology* 302(1–2):31–42.

Scourse JD, Richardson CA, Forsythe G, Harris I, Heinemeier J, Fraser N, Briffa K, Jones PD. 2006. First

cross-matched floating chronology from the marine fossil record: data from growth lines of the long-lived bivalve mollusc *Arctica islandica*. *The Holocene* 16(7):967–74.

Sherwood OA, Edinger EN. 2009. Ages and growth rates of some deep-sea gorgonian and antipatharian corals of Newfoundland and Labrador. *Canadian Journal of Fisheries and Aquatic Sciences* 66(1):142–52.

Sherwood OA, Scott DB, Risk MJ, Guilderson TP. 2005. Radiocarbon evidence for annual growth rings in the deep-sea octocoral *Primnoa resedaeformis*. *Marine Ecology Progress Series* 310:129–34.

Sherwood OA, Edinger EN, Guilderson TP, Ghaleb B, Risk MJ, Scott DB. 2008. Late Holocene radiocarbon variability in Northwest Atlantic slope waters. *Earth and Planetary Science Letters* 275(1–2):146–53.

Sikes EL, Burgess SN, Grandpre R, Guilderson TP. 2008. Assessing modern deep-water ages in the New Zealand region using deep-water corals. *Deep-Sea Research I* 55(1):38–49.

Simpson JH. 1993. Introduction to the North Sea project. *Philosophical Transactions of the Royal Society of London A* 343(1669):431–46.

Stefánsson U. 1962. North Icelandic waters. *Rit Fiskideildar* 3:1–269.

Stuiver M, Brazunias TF. 1993. Modeling atmospheric ^{14}C influences and ^{14}C ages of marine samples to 10,000 BC. *Radiocarbon* 35(1):137–89.

Stuiver M, Polach HA. 1977. Discussion: reporting of ^{14}C data. *Radiocarbon* 19(3):355–63.

Sundby S, Drinkwater K. 2007. On the mechanisms behind salinity anomaly signals of the northern North Atlantic. *Progress in Oceanography* 73(2):190–202.

Sweeney C, Gllor E, Jacobsen AR, Key RM, McKinley G, Sarmiento JL, Wanninkhof R. 2007. Constraining global air-sea gas exchange for CO_2 with recent bomb ^{14}C measurements. *Global Biogeochemical Cycles* 21(2):GB2015, doi: 10.1029/2006GB002784.

Tauber H, Funder S. 1975. ^{14}C content of recent molluscs from Scoresby Sund, central East Greenland. *Grønlands Geologiske Undersøgelese, Rapport* 75: 95–9.

Thomas H, Bozec Y, Elkalay K, de Baar HJW. 2004. Enhanced open ocean storage of CO_2 from shelf sea pumping. *Science* 304(5673):1005–8.

Toggweiler JR, Dixon K, Broecker WS. 1991. The Peru upwelling and the ventilation of the South Pacific thermocline. *Journal of Geophysical Research* 96(C11):20,467–97.

Vogel JS, Southon JR, Nelson DE, Brown TA. 1984. Performance of catalytically condensed carbon for use in accelerator mass spectrometry. *Nuclear Instruments and Methods in Physics Research B* 5(2):289–93.

Wanamaker Jr AD, Heinemeier J, Scourse JD, Richardson CA, Butler PG, Eiríksson J. 2008. Very long-lived mollusks confirm 17th century AD tephra-based radiocarbon reservoir ages for north Icelandic shelf waters. *Radiocarbon* 50(3):399–412.

Wanamaker Jr AD, Butler PG, Scourse JD, Heinemeier J, Eiríksson J, Knudsen KL, Richardson CA. 2012. Surface changes in the North Atlantic meridional overturning circulation during the last millennium. *Nature Communications* 3:899, doi:10.1038/ncomms1901.

Weidman CR. 1995. Development and application of the mollusc *Arctica islandica* as a paleoceanographic tool for the North Atlantic Ocean [unpublished PhD thesis]. Massachusetts Institute of Technology/Woods Hole Oceanographic Institution, MT/WHOI 95–20.

Weidman CR, Jones GA. 1993. A shell-derived time history of bomb ^{14}C on Georges Bank and its Labrador Sea implications. *Journal of Geophysical Research* 98(C8):14,577–88.

Weidman CR, Jones GA, Lohmann KC. 1994. The long-lived mollusk *Arctica islandica* - a new paleoceanographic tool for the reconstruction of bottom temperatures for the continental shelves of the northern North Atlantic ocean. *Journal of Geophysical Research-Oceans* 99(C9):18,305–14.

Weston K, Fernand L, Nicholls J, Marca-Bell A, Mills D, Sivyer D, Trimmer M. 2008. Sedimentary and water column processes in the Oyster Grounds: a potentially hypoxic region of the North Sea. *Marine Environmental Research* 65(3):235–49.

Witbaard R, Jenness MI, van der Borg K, Ganssen G. 1994. Verification of annual growth increments in *Arctica islandica* L. from the North Sea by means of oxygen and carbon isotopes. *Netherlands Journal of Sea Research* 33(1):91–101.

Wunsch C. 1984. An estimate of the upwelling rate in the equatorial Atlantic based on the distribution of bomb radiocarbon and quasi-geostrophic dynamics. *Journal of Geophysical Research* 89(C5):7971–8.